Effects of Single Pass and Multipass Welding on Austenitic Stainless Steel Corrosion in Aggressive Environments

Lawrence O. OSOBA[1], Joshua O. OKENIYI[2,*], Benjamin I. POGOSON[1], Omoniyi A. FASUBA[3]

[1]*Department of Metallurgical and Materials Engineering, University of Lagos, Nigeria*

[2] *Mechanical Engineering Department, Covenant University, Ota, Ogun State, Nigeria*

[3]*Materials Science and Engineering Department, African University of Science and Technology, Abuja, Nigeria*

ArticleInfo

Abstract

This study investigates single pass and multipass (three-pass) welding effects on 304 austenitic stainless steel (ASS) corrosion in acidic/saline environments, to enable a better understanding of the influence of heat affected zone (HAZ) on ASS corrosion susceptibility in the selected commonly used aggressive environments. Tungsten Inert Gas (TIG) welding process was used to weld the samples using 308 stainless steel filler. The corrosion behaviour of the welded samples was evaluated using immersion and potentiodynamic polarization tests. Immersion test evaluation and the analysed results showed that the single pass welds exhibited lower corrosion susceptibility in the acidic environments (H_2SO_4, HNO_3) than in the multipass welded ASS. In contrast, using potentiodynamic polarization evaluation, the multipass welded sample, exhibited lower corrosion susceptibility than the single pass welded ASS in HNO_3 environment. Essentially, the same trend of corrosion susceptibility was recorded in NaCl environments irrespective of the evaluation method.

1. INTRODUCTION

Welding is a well-known traditional method of fabrication and repair for many metallic alloys [1-2]. These metallic alloys include austenitic stainless steel (ASS), a material that finds usefulness in many industrial applications due to its elemental composition-induced desirable properties such as environmental compatibility, excellent corrosion resistance and relatively low cost [3-5]. Tungsten inert gas (TIG) welding is commonly used in industry for sheet joining purposes because it allows greater control over the weldment resulting in stronger and higher quality weld [6]. In addition, the process is quick, economical, clean and free of slag and sputter [7]. Generally, in a weldment or fusion joint, three distinct regions can be identified namely the fusion zone (FZ), the heat affected zone (HAZ) and the base metal [8]. The microstructure developed in the fusion zone depends on the solidification behaviour of the weld pool. Solidification occurs by a process of nucleation and growth depending on the cooling rate. As such, the FZ can be considered as a cast zone because important parameters that determine microstructures in casting, such as growth rate, temperature gradient, undercooling, and alloy composition influences microstructural development in the FZ [9].

Multipass welding in which one layer of the weld is allowed to cool before another weld is performed on top of it is commonly utilized in the industry during fabrication/joining process of thick sections, wear repair, surface hard facing or build-up. During multipass welding, the region adjacent to each new weld deposit experiences short-term high temperature (about 1300 °C) reheats [10], which cause re-melting of the previous beads, and then solidify, generating multiple heat affected zone. The heat affected zone (HAZ) in multipass weld microstructure does significantly vary from that obtained during single pass welding process because of the multiple reheats [11-12].

Correspondingauthor, joshua.okeniyi@covenantuniversity.edu.ng

Normally, the microstructure of ASS is mainly composed of austenite under equilibrium condition [13]. However, during welding, a non-equilibrium rapid solidification process due to the high cooling rate often gives rise to an incomplete transformation of austenite resulting in a small amount of delta ferrite that remain in the weld microstructure at room temperature [14-15]. The amount of retained delta ferrite is predominantly dependent on the composition of the filler metal, dilution from the parent metal and the chemical reactions that take place between the weld metal and the slag or surrounding gases. Depending on the ASS composition, ferrite, austenite, martensite or combinations of these can form due to the role of nickel and chromium in promoting the stabilization of austenite and ferrite, respectively. In addition, microstructural inhomogeneity and compositional changes occur in the HAZ adjacent to the FZ during welding. These often results in sensitization that takes the form of segregation of chromium to form $M_{23}C_6$ carbide and other inter-metallic (sigma, $Cr_{30}Mo_6Ni_5$; Chi, $Cr_{27}Mo_{12}Ni_5$ and $Cr_{20}Mo_{39}Ni_3$) phases along the grain boundaries. Sensitization, which is a major problem during high temperature processing like welding makes ASS highly susceptible to intergranular corrosion [16-18].

Although several works exist in the literature on corrosion susceptibility of ASS and the problem of its associated sensitization during welding [5,19], however, there are little and/or few information on the effects of multiple heat affected zones generated during multipass welding process on corrosion susceptibility of ASS. Also, more experimental studies are required for a better understanding of the conditions in which multipass welded stainless steel could exhibit lower corrosion susceptibility, or otherwise, than the single pass welded stainless steel. Therefore, the objective of this study was to investigate the effects of single pass and multipass welding on corrosion susceptibility of ASS in commonly used aggressive (i.e. acidic and saline) environments.

2. EXPERIMENTAL

The chemical composition of the austenitic stainless steel AISI 304 grade base plate and the 308 stainless steel filler metal used for this research is presented in Table 1.

Table 1.*Chemical composition(wt%) of the base metal and filler metal*

Type	Cr	Ni	Co	Mn	P	S	Mo	Cu	Si	Fe	C
AISI 304	18.72	7.84	0.14	1.78	0.04	0.01	0.27	0.32	0.32	70.3	0.04
(ER 308 SS)	18.15	10.01	–	1.57	0.04	0.03	–	–	1.0	69.13	0.07

The base plates were cut into sizes of 120 mm × 20 mm × 8 mm and clean with acetone to remove lubricant and surface contamination. Welding was performed using Lincoln TIG welding machine. Before welding, the base plate were machined to prepare butt joint edges chamfered at 30° and tacked at both ends of the plate to make a single vee groove of 60° while maintaining a consistent root gap of 1.5 mm. The single pass and multipass welding conditions were carried out using a 2.5 mm diameter filler electrode with a current of 100 A and arc voltage of 12 V. During and after the welding, joints were visually inspected for any geometrical non-conformity and weld defects.

Samples from the multipass and single pass welded material were cut and prepared for metallographic observation by grinding to 1200 mesh (from 120, 240, 320, 400, 600, 800 Mesh) on silicon carbide paper and finally polished on emery cloth using a suspension of alumina powder to obtain a mirror-like surface. Optical microscopy observation of the welded samples was obtained using CETI metallurgical microscope (Model No. 0703552) after the samples were etched by swabbing in a mixed solution of HCl and HNO_3 (aqua regia) in ratio 3:1 for 45 – 60 seconds.

The hardness profile of the single pass and multipass welded samples were obtained using Buehler® microhardness tester. Vickers pyramid indenter was used for microhardness measurements along the longitudinal centreline of the weld through the heat affected zone and into the base metal with a testing load of 490 mN and a dwelling time of 10 seconds.

For the immersion test, samples of sizes 40 mm × 20 mm × 8 mm were sectioned and prepared according to standard procedure prescribed in ASTM G1 [20]. The coupons were ground from 120, 240, 400, and

600 mesh silicon carbide papers and cleaned with acetone to remove grease and oxidation films, eventually rinsed in distilled water, dried and weighed. Standard grade chemicals and distilled water were used to prepare different concentrations of Sodium Chloride (NaCl) and 1 mol/dm^3 (1 M) Sulphuric Acid (H$_2$SO$_4$) and Nitric Acid (HNO$_3$) concentrations. Each of the samples was immersed in marked jars containing 200ml of corrosive test-solution for 840 hr to determine the weight loss at interval of 120 hr. The samples were removed and cleaned in distilled water and ethanol before weighing with a digital weighing machine (Uni Bloc, Type UW1020H and Model No. D482800085) that was sensitive up to 0.001 g. Each test was repeated three times to ensure the reproducibility of the test-results. The test was carried out at room temperature with no agitation and aeration.

For potentiodynamic polarization test, samples with the size of 10 mm × 10 mm × 5 mm were mounted in resin and connected with a flexible wire. The mounted samples were then ground, polished, cleaned and rinsed properly. The potentiodynamic polarization test equipment consisted of potentiostat, a stainless steel specimen as a working electrode, a platinum counter electrode and a reference electrode (saturated calomel electrode, SCE). After immersion in the solution, the polarization tests were carried out in three different concentration of sodium chloride (NaCl) and in 1 M sulphuric acid (H$_2$SO$_4$) and nitric acid (HNO$_3$) concentrations at room temperature. Data were recorded using a computer-based data logging system (Autolab PGSTAT 204N) employing NOVA software for corrosion analysis.

3. RESULTS AND DISCUSSION

3.1. Microstructural Analysis

The microstructure of the as received austenitic stainless steel as shown in Figure 1 comprises of the austenite phase and delineated grain boundaries [14].

Figure 1. *Microstructure of the as received austenitic stainless steel sample*

Optical images of the FZs and the HAZs of the welded austenitic stainless steels are shown in Figure 2a and b, for the single pass welding and the multi-pass welding, respectively. From the figure 2, microstructures of transformed zone are observed in both samples in the region close and along the fusion boundary [21]. However, the extent of transformation appears to be higher in the multipass weld bead compared to the single pass weld region.
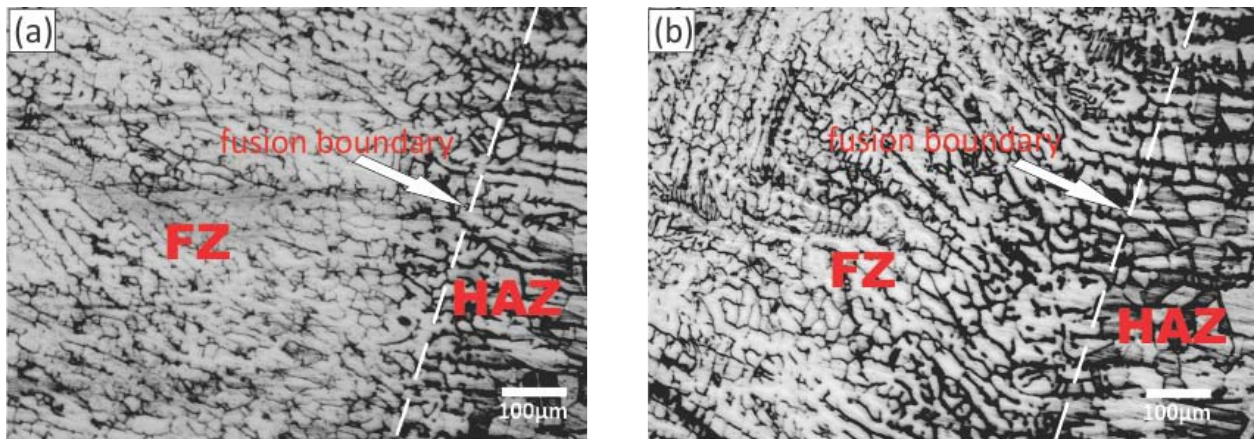
Figure 2. *Optical image of FZ and HAZ (a) single pass welded austenitic stainless steel and (b) multipass welded austenitic stainless steel*

In comparison with single pass weld metal and HAZ, the multiple HAZ generated during multipass welding is confined to the prior FZ in the welded sample. The single pass welded material appears to retain its wrought structure in the HAZ with a slight modification because of the limited heat cycle it has experienced during welding. In contrast, the multipass weld metal is significantly different in morphology due to the reheated nature of the HAZ embedded in the FZ. Furthermore, it could be observed from the optical image of the HAZ, presented in Figure 3 that the grain size in the HAZ of the single pass weld is coarse, see Figure 3a, while the grain structure in the HAZ of the multipass weld appears more refined, Figure 3b, than that from the single pass weld similar to what has been previously reported [22]. This observation may be attributed to the extent of thermal cycling and consequential recrystallization that occur during multipass welding.
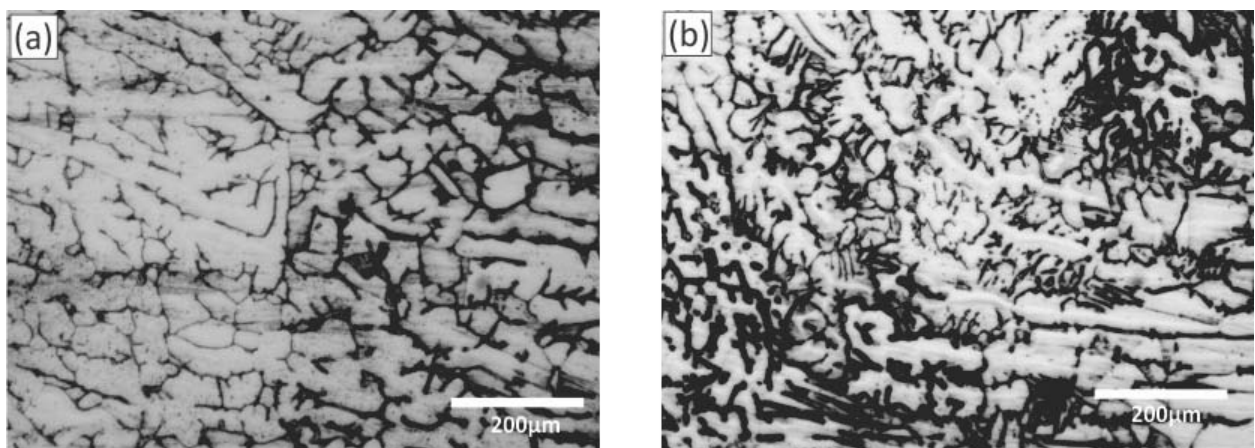
Figure 3. *Optical image of HAZ in (a) single pass welded sample (b) multipass welded sample*

Close observation of the fusion zone microstructure reveals a significant difference in the morphology of the dendritic structure in that in the single pass weld, the dendritic structure are less pronounced compared to the dense formation that occurred in the multipass weld fusion zone because of the increased number of weld passes, and it is in agreement with a previous investigation [23]. As shown in the optical image of the FZ presented in Figure 4a, for the single pass and in Figure 4b for the multipass welded sample, the fusion zone is typically dendritic with lathy ferrite morphology, similar to what has been previously reported [24].
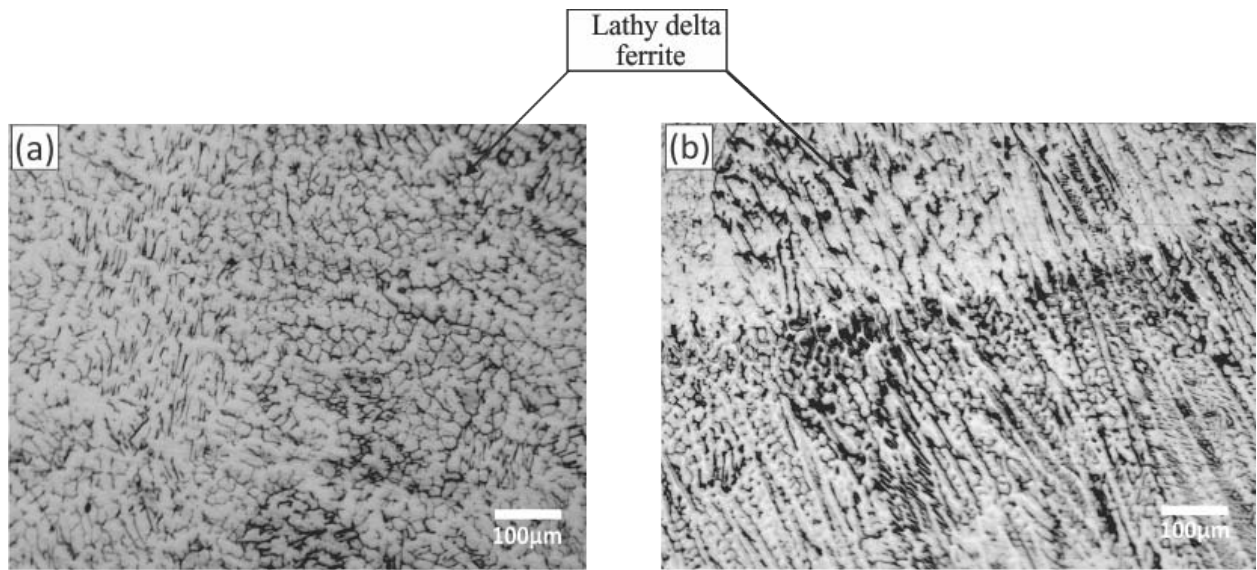
Figure 4.*Optical image of the fusion zone showing delta ferrite in (a) single pass (b) multipass welded sample*

The variation of the delta ferrite morphology in the FZ of the multipass welded sample is presented in Figure 5, which shows the optical images of the surface (Figure 5a), middle (Figure 5b) and root (Figure 5c) of the multipass welded ASS sample. Close to the surface of the FZ are more of skeletal delta ferrite as shown in Figure 5a while in the middle and close to the root of the fusion zone are more of lathy delta ferrite as shown in Figure 5b and Figure 5c, respectively. Most regions within the fusion zone have a mixed ferrite morphology [23,25-26].
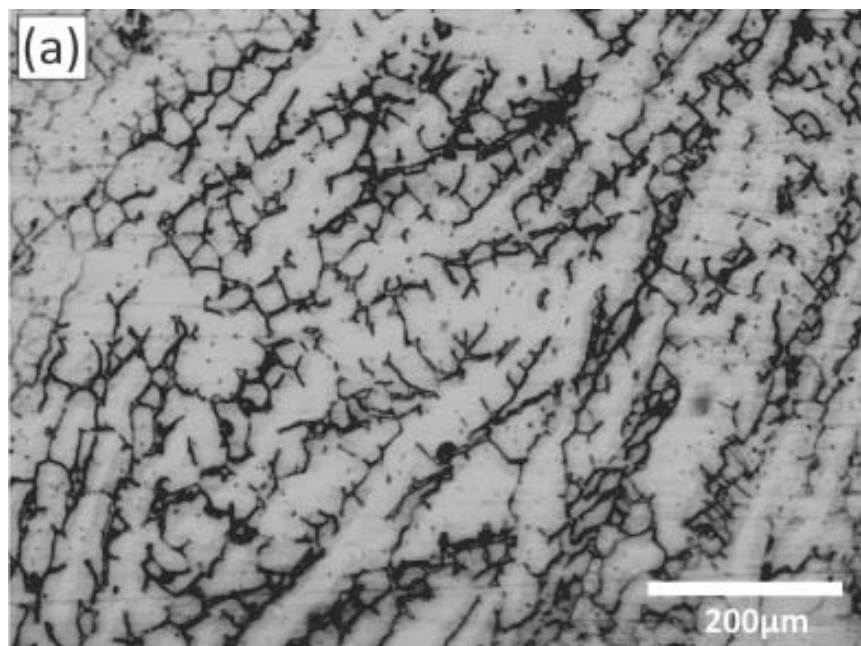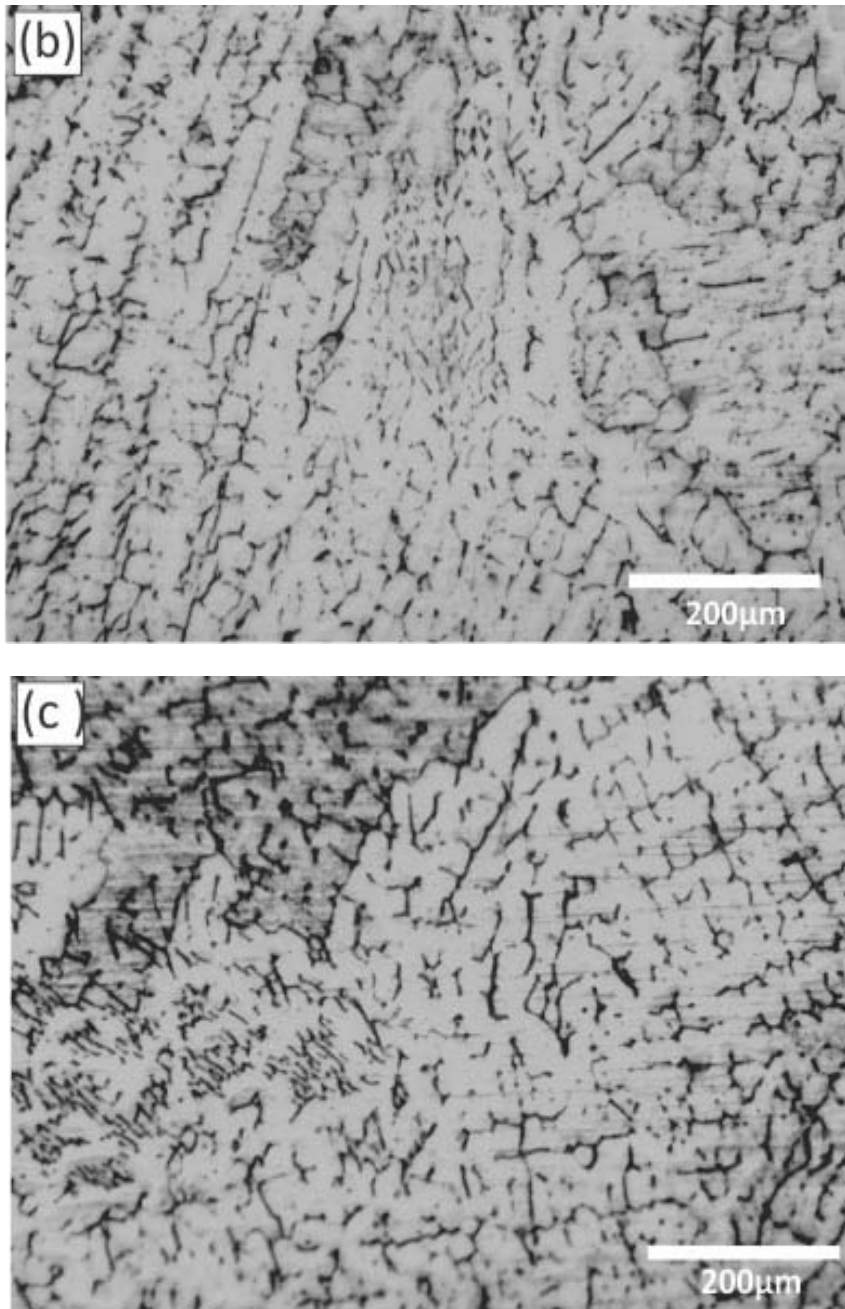
Figure 5. Optical images of the fusion zone in multipass welded samples: (a) face (b) middle (c) root

According to previous study [27], the significant effect of welding process on the microstructure that forms in the single and multipass welded material, as discussed above, is expected to have a strong influence on the corrosion susceptibility of weld metal in any aggressive environment. This is because of the significant differences in the intensity and morphology of the precipitate phases formed in the HAZs of the single pass and of the multipass weld metal.

3.2. Micro Hardness Analysis

During welding, the generation of thermally induced stresses (heating, cooling and residual) is inevitable owing to the expansion and contraction that occurred during the process [21,28-29]. One of the factors that could possibly alter the susceptibility of welded structure to corrosion is the magnitude of the induced stresses that emanated during welding, which can be related to the microhardness that developed across the weld joint. Therefore, the results of the microhardness evaluation of HAZ in the single pass and the multiple HAZ in the multipass welded materials for this study are presented in Figure 6.
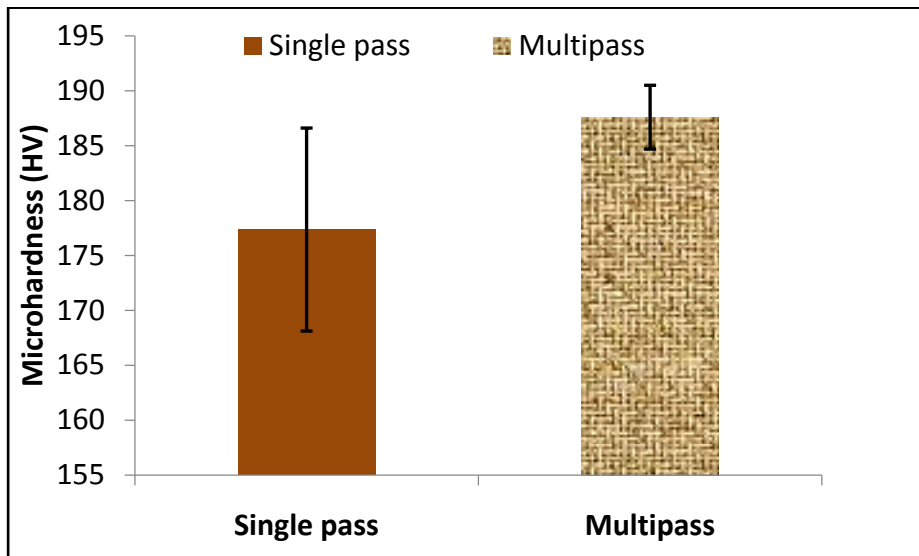
Figure 6.*Microhardness of the HAZ in single pass and multiple heat affected zone in multipass welded samples*

The results show that the hardness in the heat affected zone of the multipass welded material is higher than that in the HAZ of the single pass welded material [23,28]. This result further supports the formation of retransformed nature of the microstructure formed in the multipass weld metal compared to the essentially coarser microstructure in the single pass welded material. Based on the microhardness results, its influence on corrosion susceptibility of the multipass welded sample and the coarse microstructure observed in the single pass weld was investigated in acidic (H_2SO_4, HNO_3) and basic (NaCl) environment.

3.3. Corrosion Behaviour

3.3.1. Immersion tests and analyses

The results of corrosion susceptibility evaluation are presented in Figure 7 for the single pass and the multipass welded ASS materials immersed in different test-environments including 1 M HNO_3 (Figure 7a), 1 M H_2SO_4 (Figure 7b) and 1 M NaCl (Figure 7c) test-solution. From the figure, it is observed that corrosion rate decreases with exposure time in all the test-environments. This can be attributed to the formation of an impervious thin layer of oxide on the surface of the ASS in each corrosive medium that slows down or prevents further attack by the corrosive media [30-32].
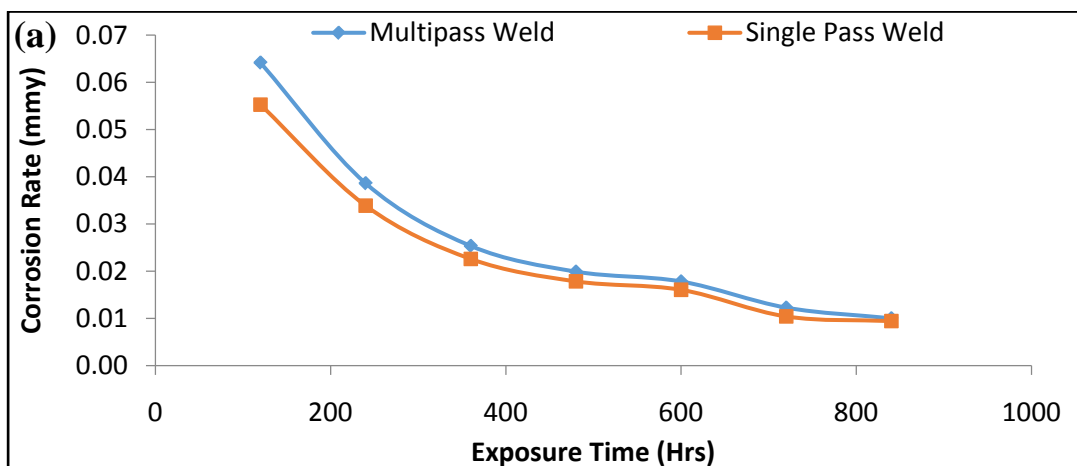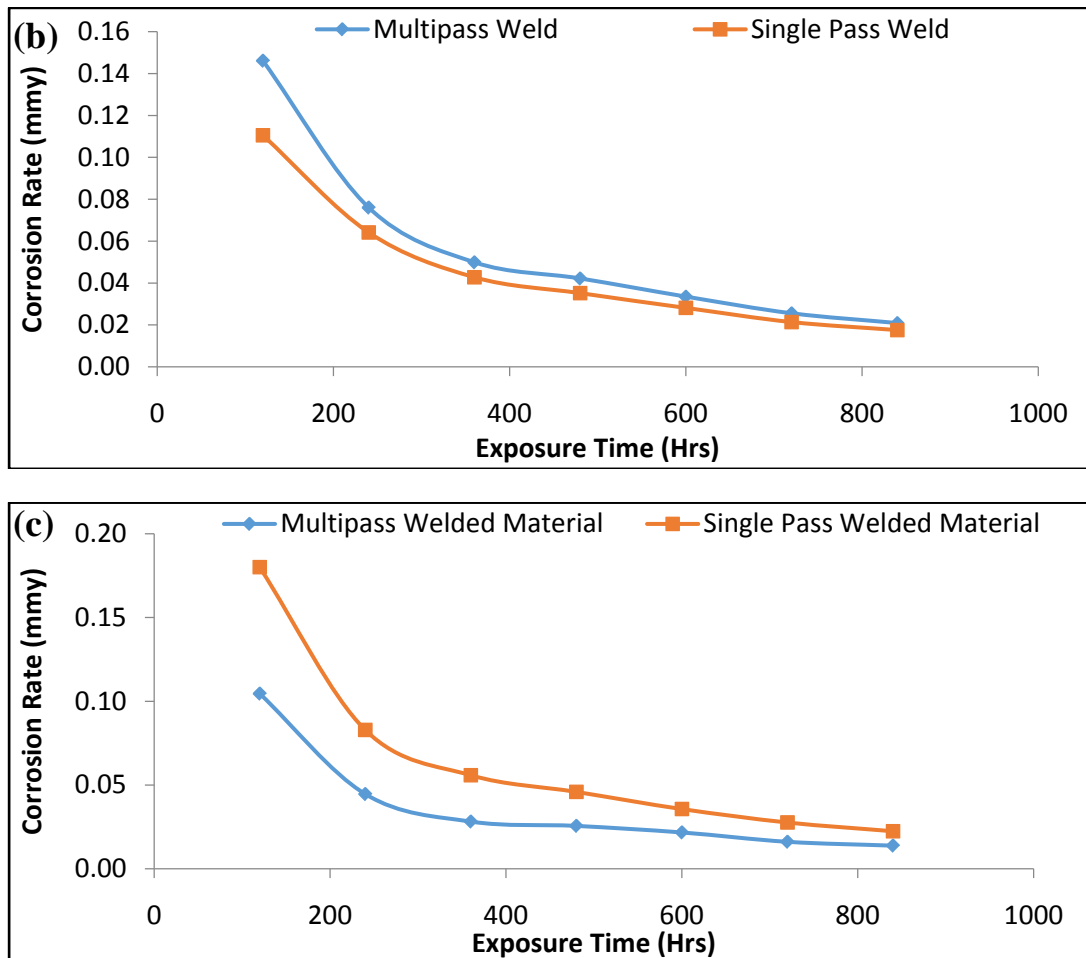
Figure 7. *Corrosion effect of single pass and multipass welded ASS immersed in test-solutions of (a) 1 M NNO₃, (b) 1 M H₂SO₄ and (c) 1M NaCl*

Numerical detailing of the corrosion test-results through correlation fitting analyses of corrosion rate, *CR*, as dependent variable [33] versus exposure time, *t*. Independent variable shows that the corrosion test-responses from the 1 M HNO₃ test-system followed the relationships:

$$CR_{\text{single pass (HNO}_3)} = 10^{-3}\left[6354.46\left(1/t\right) + 4.01\right] \tag{1}$$

$$CR_{\text{multipass (HNO}_3)} = 10^{-3}\left[7453.84\left(1/t\right) + 3.87\right] \tag{2}$$

For these correlation fitting models, correlation coefficient, R, and the Nash-Sutcliffe efficiency, NSE, [34] are respectively 99.10% and 98.21% for the single pass (Equation (1)) or 99.27% and 98.55% for the multipass (Equation (2)) welded ASS samples in the 1 M HNO3 test-medium. These correlation parameters interpret to excellent fitting model efficiency by both of the correlation fitting relationships [35-36]. From the correlation fitting Equation (1) and Equation (2), it could be deduced that the multipass welded ASS metal exhibited slightly higher rate of corrosion susceptibility than the single pass welded ASS, especially at low exposure time. However, this disparity in corrosion susceptibility is so small that increase in exposure time could quickly culminate in similarity of corrosion test-responses by both the single pass and the multipass welded ASS material, which is what is observable from the test-results plotted in Figure 7a.

In similar manner, the corrosion test-responses from the 1 M H₂SO₄ test-system followed the relationships:

$$CR_{\text{single pass (H}_2\text{SO}_4)} = 10^{-3}\left[12{,}821.36(1/t) + 6.11\right] \tag{3}$$

$$CR_{\text{multipass (H}_2\text{SO}_4)} = 10^{-3}\left[17{,}253.96(1/t) + 3.06\right] \tag{4}$$

The respective parameters (R, NSE) for these fitting models are (99.56%, 99.12%) for the single pass (Equation(3)) or (99.89%, 99.78%) for the multipass (Equation(4)) welded ASS material immersed in the 1 M H_2SO_4 test-solution. Also, these parameters interpret to excellent model efficiency by the correlation fitting models of Equation (3) and Equation (4). The correlation fitting models also showed that the multipass welded ASS exhibited higher rate of corrosion susceptibility in the H_2SO_4 medium, at given exposure time, which is even of higher order than was observed with the HNO_3 test-system. This contrast followed from the well-known tendency of nitric acid (HNO_3) at forming passive film on the surfaces of materials exposed to it, although it also known that should such passive film be broken, abrupt change in corrosion rate could ensue. For the H_2SO_4 solution, the multipass welded ASS attains high corrosion rate faster than the single pass welded ASS, although, the disparity in corrosion rate still exhibit tendency of disappearing with increasing exposure time, as could also be observed in Figure 7b.

The corrosion test-responses from the 1 M NaCl test-solution assumed the relationships:

$$CR_{\text{single pass (NaCl)}} = 10^{-3}\left[21{,}694.58(1/t) - 2.63\right] \tag{5}$$

$$CR_{\text{multipass (NaCl)}} = 10^{-3}\left[12{,}494.17(1/t) - 2.25\right] \tag{6}$$

These exhibited correlation parameters (R, NSE) that respectively evaluate to (99.87%, 99.74%) for the single pass (Equation(5)) or (99.43%, 98.87%) for the multipass (Equation(6)) welded metal immersed in the 1 M NaCl test-solution. These are parameter values that also indicate excellent fitting model efficiency by the correlation equations. In contrast to the previous results, however, the correlation fitting models showed that the multipass welded ASS exhibited much lesser rate of corrosion susceptibility at given exposure time than the single pass welded ASS material in the 1 M NaCl test-environment. The single pass welded ASS corrodes faster than the multipass welded ASS in the 1 M NaCl. This is well corroborated by the experimental corrosion test results plotted in Figure 7c.

Based on the foregoing results and consequent interpretations, it is considered appropriate to study analyses of variance (ANOVA). This is to enable the testing significance of the obtained correlated relationships between the dependent variable, CR, and independent variable, t. Based on the results from previous ANOVA studies [33,37] and presented for the test-systems of 1 M HNO_3 in Table 2, for 1 M H_2SO_4 in Table 3 and of 1 M NaCl in Table 4. The results in the tables showed that p-value is $\ll 0.05$ for each of the test-systems, an indication that a significant relationships exist between the dependent variable CR and t, for each of the test systems of 1 M HNO_3, 1 M H_2SO_4, and 1 M NaCl.

Table 2. *Analyses of variance for the correlation fitting from the 1 M HNO₃ test-system*

ASS Welded Model	Source of Variation	df	SS	MS	F	p-value
Single Pass	Treatment	1	1.5461×10^{-3}	1.5461×10^{-3}	274.4541	**1.46×10^{-5}**
	Residual	5	2.8167×10^{-5}	5.6335×10^{-6}		
	Total	6	1.5743×10^{-3}			
Multipass	Treatment	1	2.1274×10^{-3}	2.1274×10^{-3}	339.2703	**8.68×10^{-6}**
	Residual	5	3.1353×10^{-5}	6.2705×10^{-6}		
	Total	6	2.1588×10^{-3}			

Table 3. *Analyses of variance for the correlation fitting from the 1 M H$_2$SO$_4$ test-system*

ASS Welded Model	Source of Variation	df	SS	MS	F	p-value
Single Pass	Treatment	1	6.2945×10^{-3}	6.2945×10^{-3}	566.3693	**2.44×10^{-6}**
	Residual	5	5.5568×10^{-5}	1.1114×10^{-5}		
	Total	6	6.3500×10^{-3}			
Multipass	Treatment	1	1.1399×10^{-2}	1.1399×10^{-2}	2244.9552	**7.91×10^{-8}**
	Residual	5	2.5388×10^{-5}	5.0776×10^{-6}		
	Total	6	1.1424×10^{-2}			

Table 4. *Analyses of variance for the correlation fitting from the 1 M NaCl test-system*

ASS Welded Model	Source of Variation	df	SS	MS	F	p-value
Single Pass	Treatment	1	1.8022×10^{-2}	1.8022×10^{-2}	1928.6347	**1.16×10^{-7}**
	Residual	5	4.6721×10^{-5}	9.3442×10^{-6}		
	Total	6	1.8068×10^{-2}			
Multipass	Treatment	1	5.9773×10^{-3}	5.9773×10^{-3}	438.1099	**4.61×10^{-6}**
	Residual	5	6.8217×10^{-5}	1.3643×10^{-5}		
	Total	6	1.1424×10^{-2}			

Figure 8 shows the results of average corrosion rate evaluations for the single pass and the multipass welded ASS material in the different test-immersion environments of 1 M HNO$_3$, 1 M H$_2$SO$_4$ and 1 M NaCl. This figure vividly highlights the slight disparity in the corrosion susceptibility in HNO$_3$, the higher disparity in corrosion susceptibility in H$_2$SO$_4$, and the contrasting change in corrosion susceptibility behaviour in NaCl by the single pass and the multipass welded ASS metal.
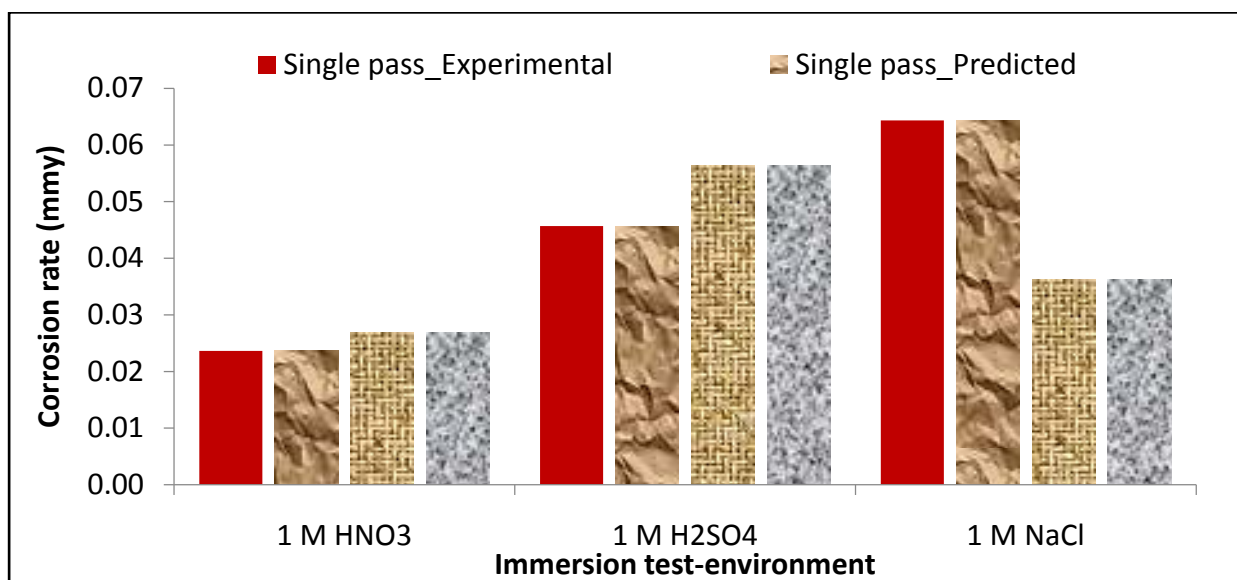
Figure 8. *Experimental and predicted average corrosion rate of single pass and multipass welded austenitic stainless steel in different immersion environments*

The observed tendency of reduced corrosion susceptibility in the NaCl test-environment is investigated in this study by varying the concentrations of NaCl test-solution (using 0.5 M NaCl and the 0.75 M) for immersion test of the single pass and the multipass welded ASS material, in addition to the 1 M NaCl.

The results of corrosion susceptibility evaluation in these additional concentrations of NaCl test-environments is presented in Figure 9, i.e. Figure 9a and 9b for the 0.5 M NaCl and 0.75 M NaCl test-systems, respectively. From figure 9, it is noted that the trend of decreasing corrosion rate with increasing exposure time, as previously reported above from all the corrosion test-environments, also predominates. Furthermore, in agreement with observed results from the 1 M NaCl test-environment as seen in Figure 7c, Figure 9 showed that the corrosion rate for the single pass welded ASS are consistently higher than that of the multipass welded ASS in both the 0.5 M NaCl and the 0.75 M NaCl test-environment. The results confirm that the multipass welding procedure do not degrade the corrosion resistant property of the ASS material in the NaCl environment, but rather exhibited an apparent improvement in the corrosion resistant property compared to the single pass welded metal in the same environment.
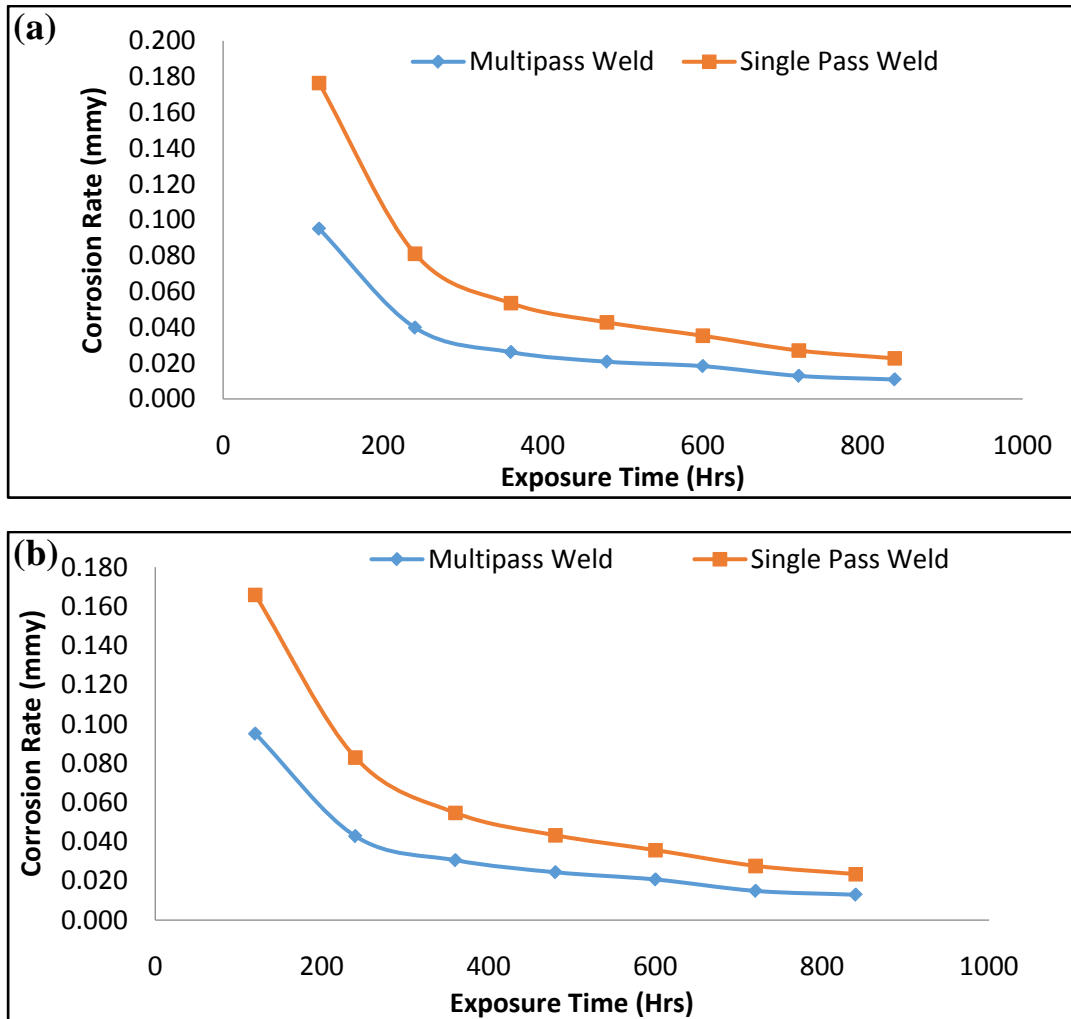
Figure 9. *Corrosion effect of multipass and single pass welded ASS in (a) 0.5M NaCl (b) 0.75M NaCl*

The lower corrosion rate, *CR*, by the multipass welded ASS than that from the single pass material, for given NaCl concentration, ρ, and immersion time, *t*, is further corroborated by the correlation fitting Equation (7) for the single pass and Equation (8) for the multipass model. For these fittings, the corrosion rate, taken as dependent variable [33], was correlated with functions of the concentration, ρ, of the NaCl test-solution (including the 1 M NaCl system) and of the immersion time, *t*, taken as the independent variables, for obtaining the relationships:

$$CR_{\text{single pass}} = 10^{-3}\left[41.41\rho + 0.2t + \ln\left(\rho^{-27.49} \cdot t^{-146.96}\right) + 809.27\right] \tag{7}$$

$$CR_{\text{multipass}} = 10^{-3}\left[1.62\rho + 0.13t + \ln\left(\rho^{5.09} \cdot t^{-87.4}\right) + 498.71\right] \quad (8)$$

From these correlation fitting equations, it is deduced that, for given NaCl concentration, higher value of corrosion rate will be initiated faster in the single pass welded material than in the multipass welded material. These suggest a faster corrosion failure tendency by the single pass welded ASS than the multipass welded ASS. Furthermore, it is worth noting that the correlation coefficient, *R*, and the Nash-Sutcliffe efficiency, *NSE*, for the correlation fittings in Equation (7) and Equation (8), are respectively 99.26% and 98.53% for the single pass model, 98.75% and 97.52% for the multipass model. These fitting parameters also indicate an excellent model efficiency by each of the correlation models based on previous work [35-36]. The analyses of variance for the correlation fittings, shown in Table 5, indicate that ANOVA *p*-values << 0.05 for both of the welded models, which implies that it could not be rejected that there is significant relationship between the dependent and independent variables, for the models.

Table 5. *Analyses of variance for the correlation fitting from the different NaCl test-systems*

ASS Welded Model	Source of Variation	*df*	SS	MS	F	*p*-value
Single Pass	Treatment	4	0.0497	0.0124	268.2739	1.93×10^{-14}
	Residual	16	7.4119×10^{-4}	4.6324×10^{-5}		
	Total	20	0.0505			
Multipass	Treatment	4	0.0158	3.9516×10^{-3}	157.1677	1.27×10^{-12}
	Residual	16	4.0228×10^{-4}	2.5142×10^{-5}		
	Total	20	0.0162			

The average corrosion rate of the single pass and of the multipass welded ASS by the experimental model and the predicted model from the correlation fitting are presented in Figure 10, for the different concentrations of NaCl test-solutions employed in the study. This also includes the average corrosion rate from the 1 M NaCl test-system, for fostering comparisons across the different concentrations of NaCl employed for the study. By these, it could deduced from the Figure 10 that the predicted model exhibited agreements with the experimental model and both of these models further confirmed that the multipass ASS welded materials exhibited lower corrosion susceptibility than the single pass ASS welded materials in the NaCl environment.
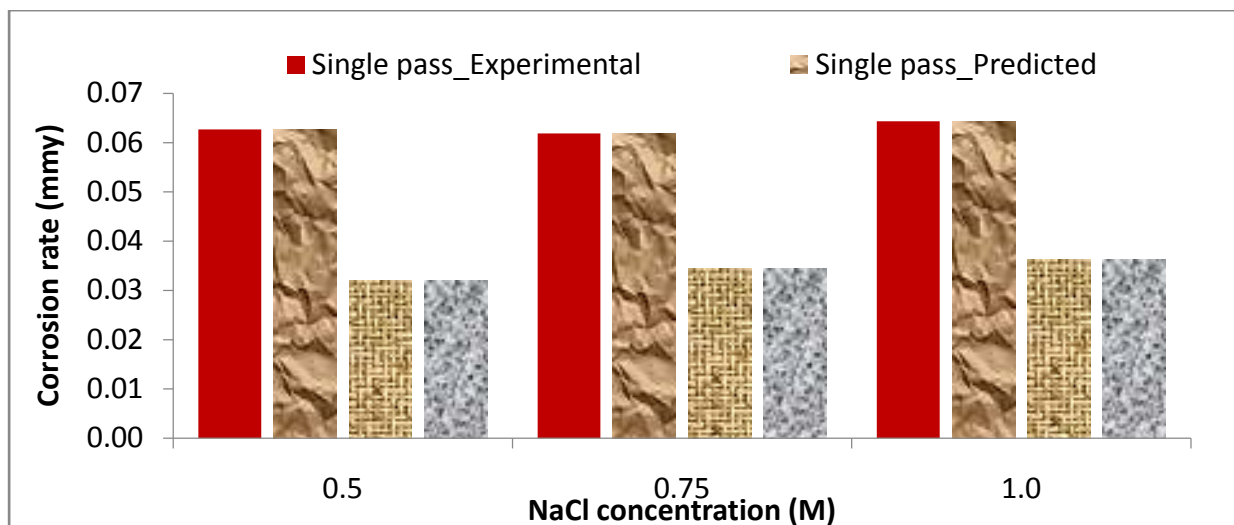
Figure 10. *Experimental and predicted average corrosion rate of single pass and multipass welded austenitic stainless steel in varying concentration of NaCl*

3.3.2. Corrosion rate by potentiodynamic polarization test

In order to verify and clarify the observed results from immersion test, potentiodynamic polarization measurements was carried out, because it is a fast, simple and reliable ways of selecting/evaluating corrosion susceptibility of materials in specific environment. The plots from these potentiodynamic test-experiments are presented in Figure 11, for the 1 M HNO_3, the 1 M H_2SO_4, the 1 M NaCl and the 0.5 M NaCl corrosive test-systems. In addition, results of the corrosion current density (i_{corr}), corrosion potential (E_{corr}) and polarization resistance for each of the tested ASS samples were determined for each medium from the potentiodynamic polarization curves (using Tafel extrapolation method). These results are summarized in Table 6.
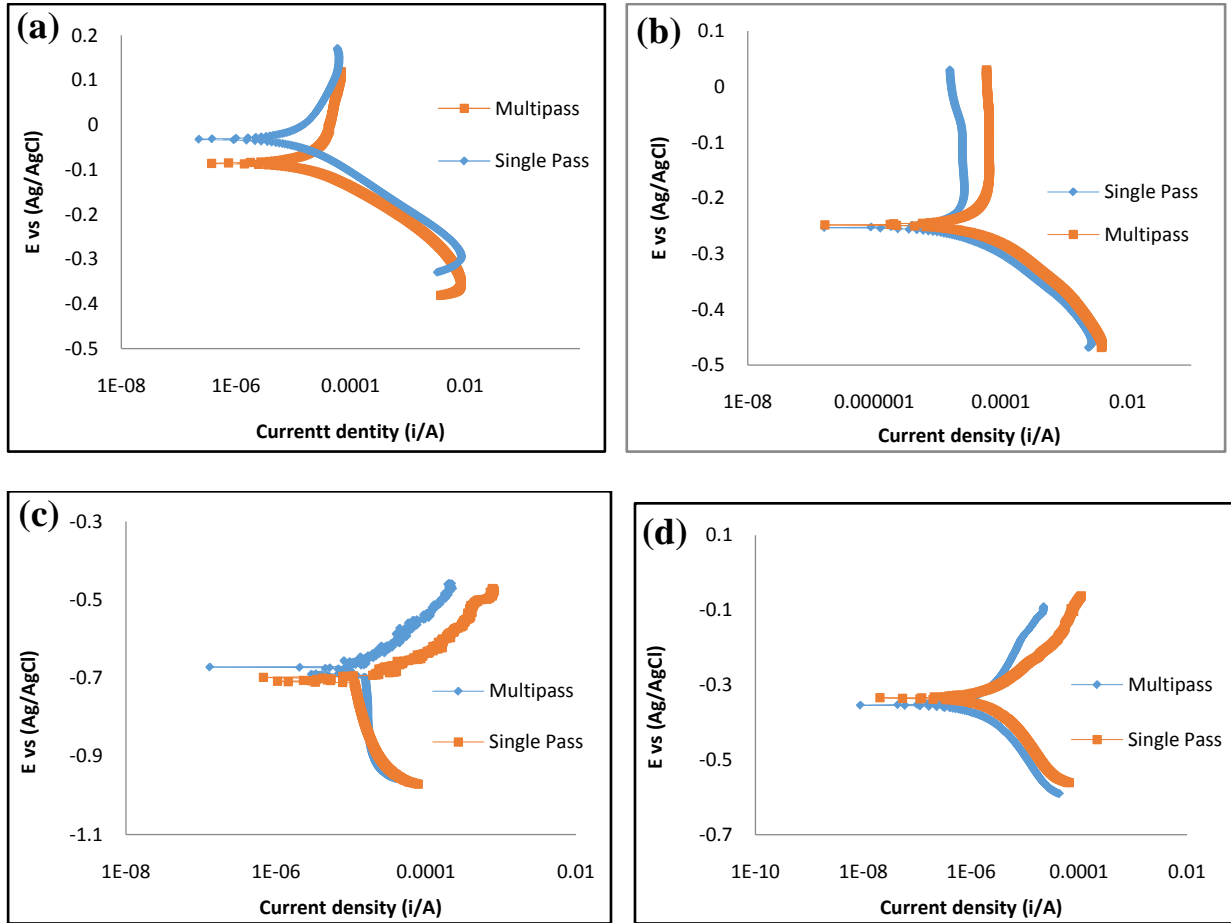
Figure 11. *Potentiodynamic polarization curves of single pass and multipass welded austenitic stainless steel in (a) 1 M HNO₃ (b) 1 M H₂SO₄ (c) 1 M NaCl (d) 0.5 M NaCl solution*

Table 6. *Electrochemical corrosion parameters obtained from potentiodynamic polarization curves for various samples in varying concentration and media*

Corrosive test-system	i_{corr} (µA/cm^2)		E_{corr} (mV)		Polarization Resistance (Ω)	
	Single Pass	Multipass	Single Pass	Multipass	Single Pass	Multipass
1M HNO_3	18.80	16.80	−32.11	−86.01	1712.40	1019.20
1M H_2SO_4	27.63	69.58	−252.99	−267.85	512.82	506.62
1M NaCl	0.502	0.132	−708.91	−672.21	3547.60	1243.10
0.5M NaCl	2.37	1.15	−334.92	−353.67	11889.00	19420.00

The potentiodynamic polarization test-results followed the trend observed in the immersion corrosion tests evaluation, with an exception of corrosion susceptibility in the HNO_3 test- environment. In contrast

to the results obtained from the immersion test, the multipass welded ASS exhibited lower corrosion susceptibility than the single pass welded sample, as observed in the value of the corrosion current density, 16.80 µA/cm^2 which is rather lower than that observed in single pass 18.80 µA/cm^2 although the polarization resistance is comparably higher in multipass weld. . This observation may be related to the inequality in the degree of passivation experience by multipass and the single pass welded ASS in HNO$_3$ environment during potentiodynamic tests. The corrosion potential confirms this suspicion of passivation disparity, especially, from the consideration that although the corrosion current density of the multipass welded ASS was lower, its corrosion potential was more negative than what was obtained from the single pass welded ASS. From the remaining tests, however, the following agrees with the results from the immersion test-method ensued:

   i.   The multipass welded ASS exhibited higher corrosion susceptibility than the single pass welded ASS in the 1 M H$_2$SO$_4$ test-environment based on all parameters of corrosion current density, polarization resistance and corrosion potential;

   ii.   The multipass welded ASS exhibited lower corrosion susceptibility than the single pass welded ASS in the 1 M NaCl test-environment based on corrosion current density and the corrosion potential considerations;

   iii.   The multipass welded ASS exhibited lower corrosion susceptibility than the single pass welded ASS in the 0.5 M NaCl test-environment based on all parameters of corrosion current density, the polarization resistance and corrosion potential.

The influence of multiple heat affected zone occurrence due to multipass welding using immersion and potentiodynamic polarization test shows that the practice of multipass welding does not negatively aggravate corrosion sensitization of austenitic stainless steel weld metal in NaCl and in HNO$_3$ environments. This observation may be attributed to the role of elemental chromium segregation on corrosion susceptibility in wrought ASS where the microstructure in the HAZ of single pass welded material is influenced by the formation of M$_{23}$C$_6$ along grain boundaries [38-39]. The as-cast delta ferrite precipitate phase in the multiple HAZ embedded in the FZ of the multipass weld appears to have considerable influence its susceptibility to corrosion. In essence, in the single pass welding process, the wrought microstructure of the HAZ where M$_{23}$C$_6$ precipitates are formed owing to chromium segregation and are known to cause sensitization with associated degradation of corrosion resistance. Furthermore, as observed in the current study, the multipass welded material have a significant delta ferrite precipitation in the multiple HAZ embedded in FZ compared to the single pass weld metal. In addition, the multiple heat affected zone can possibly lead to preheating and homogenization of the previous weld pass in the multipass welded samples and this may also have contributed to the improvement in the corrosion resistance and passivity with time in the multipass weld metal.

4. CONCLUSİON

In this study, single pass and multipass welded austenitic stainless steel samples were used to investigate the influence of heat affected zone produced during the welding on the corrosion susceptibility of austenitic stainless steel. From the results in the study, it can be concluded that:

- The multipass weld metals have a significant delta ferrite morphology precipitation compared to the single pass welded material having a wrought alloy microstructure;
- The multipass welded material has a comparatively higher hardness value in the fusion zone and heat affected zone compared to the single pass welded material;
- Analysed corrosion test-results detailed corrosion susceptibility and exhibited results that agreed with experimental results;
- Experimental and analysed corrosion test-results showed that although the single pass welded ASS exhibited lower corrosion susceptibility in H$_2$SO$_4$ than the multipass welded ASS, however, the multipass welded ASS exhibited lower corrosion susceptibility in NaCl environments, as well as in the HNO$_3$ test-environment using the evaluation.
- These results indicated that the practice of multipass welding does not necessarily aggravate corrosion susceptibility of austenitic stainless steel material in HNO$_3$ and in NaCl.

CONFLICTS OF INTEREST

No conflict of interest was declared by the authors.

REFERENCES

[1] Moteshakker, A.,Danaee, I., "Microstructure and corrosion resistance of dissimilar weld-joints between duplex stainless steel 2205 and austenitic stainless steel 316L" Journal of Materials Science & Technology, 32(3): 282–290, (2016).

[2] Sule, J., Ganguly, S., Coules, H., Pirling, T. "Application of local mechanical tensioning and laser processing to refine microstructure and modify residual stress state of a multi-pass 304L austenitic steels welds", Journal of Manufacturing Processes,18: 141–150, (2015).

[3] Köse, C., Kaçar, R., Zorba, A.P., Bağırova, M., Allahverdiyev, A.M., "The effect of CO_2 laser beam welded AISI 316L austenitic stainless steel on the viability of fibroblast cells, in vitro", Materials Science and Engineering: C,60: 211–218, (2016).

[4] Cai, Y., Luo, Z., Feng, M., Liu, Z., Huang, Z., & Zeng, Y., "Effect of activator on mechanical properties and intercrystalline corrosion resistance of austenitic stainless steel weld", Journal of Materials Processing Technology, 234: 243-248, 2016.

[5] McGuire M.F., Stainless Steels for Design Engineers, ASM International, Materials Park, OH,(2008).

[6] Kurt, H.İ.,Samur, R., "Study on microstructure, tensile test and hardness 304 stainless steel jointed by TIG welding", International Journal of Science and Technology, 2(2): 163–168, (2013).

[7] Devakumar, D.,Jabaraj, D.B., "Research on gas tungsten arc welding of stainless steel-An overview", International Journal of Scientific & Engineering Research, 5(1): 1612–1618, (2014).

[8] Cary, H. B.,Helzer S.C., Modern Welding Technology 6th ed., Prentice Hall, NJ, (2005).

[9] Sindo, K., Welding Metallurgy 2nd ed., John Wiley &Sons Inc., NJ, (2003).

[10] Murugan S., Kumar P.V., Raj B., and Bose M.S.C., "Temperature distribution during multipass welding of plates", International Journal of Pressure Vessels and Piping, 75(12): 891–905, (1998).

[11] Gowrisankar, I., Bhaduri, A.K., Seetharaman, V., Verma, D.D.N., Achar, D.R.G., "Effect of the number of passes on the structure and properties of submerged arc welds of AISI type 316L stainless steel", Welding Jurnal, 147–154s, (1987).

[12] Gadewar, S.P., Swaminadhan, P., Harkare, M.G., Gawande, S.H., "Experimental investigations of weld characteristics for a single pass TIG welding with SS304", International Journal of Engineering Science and Technology,3676–3686, (2010).

[13] Marshall, P., Austenitic Stainless Steels; Microstructure and Mechanical Properties, Elsevier Applied Science Publishers Ltd, Essex, England, (1984).

[14] Shankar, V., Gills, T.P.S., Mannan S.L., Sundaresan, S., "Solidification cracking in austenitic stainless steel welds", Sadhana, 28(3-4):359–382, (2003).

[15] Padilha, A.F, Tavares, C.F.,Martorano, M.A., "Delta ferrite formation in austenitic stainless steel castings", Materials Science Forum, 730-732: 733–738, (2013).

[16] Laleh, M., Kargar, F., Rouhaghdam, A.S., "Prevention of weld-decay in austenitic stainless steel by using surface mechanical attrition treatment", International Nano Letters, 2(1): 1–6, (2012).

[17] Garcia, T.C., de Tiedra, M.P., Blanco, Y., Martin, O., Martin, F., "Intergranular corrosion of welded joints of austenitic stainless steels studied by using an electrochemical minicell", Corrosion Science, 50(8): 2390-2397, (2008).

[18] ASM International. Corrosion of Weldment; ASM Metal Handbook, Corrosion, 9th ed. Vol 13, ASM International, Materials Park, OH,771–837, (1987).

[19] Vignal, V., Richoux, V., Suzon, E., Thiébaut, S., Tabaleiv, K., "The use of potentiostatic pulse testing to study the corrosion behavior of welded stainless steels in sodium chloride solution", Materials & Design, 88: 186–195, (2015).

[20] ASTM G1-03. Standard practice for preparing, cleaning, and evaluating corrosion test specimens, ASTM International, West Conshohocken, PA, (2011).

[21] Wang, J., Lu, S., Rong, L., Li, D., "Thermal cycling, microstructure and mechanical properties of 9Cr2WVTa steel welds", Journal of Materials Processing Technology, 222: 434–443, (2015).

[22] Chen X., Chen X., Xu, H., and Madigan B., "Monte Carlo simulation and experimental measurements of grain growth in the heat affected zone of 304 stainless steel", International Journal of Advanced Manufacturing, 80(5-8): 1197–1211, (2015).

[23] Hsieh C., Lin D., Chen M., and Wu W., "Microstructure, recrystallization, and mechanical property evolutions in the heat-affected and fusion zones of the dissimilar stainless steels", Materials Transactions, 48(11): 2898–2902, (2007).

[24] Mirshekari, G.R., Tavakoli, E., Atapour, M., Sadeghian, B., "Microstructure and corrosion behavior of multipass gas tungsten arc welded 304L stainless steel", Materials & Design, 55: 905–911, (2014).

[25] Dadfar M., Fathi M.H., Karimzadeh F., Dadfar M.R., and Saatchi A., "Effect of TIG welding on corrosion behavior of 316L stainless steel",Materials Letters, 61(11, 12): 2343–2346, (2007).

[26] Ahmadi, E., Ebrahimi, A.R., Khosroshahi, A., "Welding of 304L stainless steel with activated tungsten inert gas process (A-TIG)", International Journal of ISSI, 10(1): 27–33, (2013).

[27] David, S.A., Babu, S.S., Vitek, J.M., "Welding: Solidification and microstructure", JOM, 55(6): 14–20, (2003).

[28] Kumar, D.H., and Reddy A.S., "Study of mechanical behaviour in austenitic stainless steel 316 LN welded joints", International Journal of Mechanical Engineering and Robotics Research, 2(1): 37–56, (2013).

[29] Chougule, M., Unhale, M., Walunj, A., Chavhan S., Somase, S., "Study of thermally induced residual stresses for stainless steel grade using GMAW process",International Journal of Technology Enhancements and Emerging Engineering Research, 2(6): 17–25, (2014).

[30] Iliyasu, I., Yawas, D.S., Aku S.Y., "Corrosion behaviour of austenitic stainless steel in sulphuric acid at various concentration", Advances in Applied Science Research, 3(6): 3909–3915, (2012).

[31] Loto, R.T., Loto, C.A., Popoola P.A.I., Ranyaoa M., "Corrosion resistance of austenitic stainless steel in sulphuric acid", International Journal of Physical Sciences, 7(10): 1677 – 1688, (2012).

[32] Iyasara, A. C.,Ovri, J.E.O., "Corrosion inhibition of stainless steel (314L) using molasses", The International Journal of Engineering Science, 2(1): 346–352, (2013).

[33] Okeniyi, J.O., Ambrose, I.J., Okpala, S. O., Omoniyi, O.M., Oladele, I.O., Loto, C.A., Popoola, P.A.I., "Probability density fittings of corrosion test-data: Implications on $C_6H_{15}NO_3$ effectiveness on concrete steel-rebar corrosion", Sadhana, 39(3): 731–764, (2014).

[34] Okeniyi, J.O., Ambrose, I.J., Oladele, I.O., Loto, C.A., Popoola, P.A.I., Electrochemical performance of sodium dichromate partial replacement models by triethanolamine admixtures on steel-rebar corrosion in concretes", International Journal of Electrochemical Science, 8: 10758–10771, (2013).

[35] Okeniyi, J.O., Loto, C.A., Popoola, A.P.I. "Electrochemical performance of *Anthocleista djalonensis* on steel-reinforcement corrosion in concrete immersed in saline/marine simulating-environment", Transactions of the Indian Institute of Metals, 67(6): 959–969, (2014).

[36] Coffey, R., Dorai-Raj, S., O'Flaherty, V., Cormican, M., Cummins, E., "Modeling of pathogen indicator organisms in a small-scale agricultural catchment using SWAT", Human and Ecological Risk Assessment: An International Journal, 19(1): 232–253, (2013).

[37] Okeniyi, J.O., Oladele, I.O., Ambrose, I.J., Okpala, S.O., Omoniyi, O.M., Loto, C.A., Popoola, A.P.I. "Analysis of inhibition of concrete steel-rebar corrosion by $Na_2Cr_2O_7$ concentrations: Implications for conflicting reports on inhibitor effectiveness", Journal of Central South University, 20(12): 3697–3714, (2013).

[38] Lin, C.M., Tsai, H.L., Cheng, C.D., Yang, C., "Effect of repeated weld-repairs on microstructure, texture, impact properties and corrosion properties of AISI 304L stainless steel", Engineering Failure Analysis, 21: 9–20, (2012).

[39] AghaAli, I., Farzam, M., Golozar, M.A., Danaee, I., "The effect of repeated repair welding on mechanical and corrosion properties of stainless steel 316L", Materials & Design, 54: 331–341, (2014).